

Physical properties of $R\text{Bi}_2$ ($R = \text{La}, \text{Ce}$) under pressure

Li Xiang,^{1,2} Elena Gati,^{1,2} Kathryn Neilson,² Sergey L. Bud'ko,^{1,2} and Paul C. Canfield^{1,2}

¹*Ames Laboratory, Iowa State University, Ames, Iowa 50011, USA*

²*Department of Physics and Astronomy, Iowa State University, Ames, Iowa 50011, USA**

(Dated: July 23, 2019)

We present a study of electrical transport properties of $R\text{Bi}_2$ ($R = \text{La}, \text{Ce}$) under hydrostatic pressure up to ~ 2.5 GPa. These measurements are complemented by thermodynamic measurements of the specific heat on CeBi_2 at different pressures up to 2.55 GPa. For CeBi_2 , we find a moderate increase of the antiferromagnetic transition, T_N , from 3.3 K to 4.4 K by pressures up to 2.55 GPa. Notably, resistance measurements for both CeBi_2 and LaBi_2 show signatures of superconductivity for pressures above ~ 1.7 GPa. However, the absence of superconducting feature in specific heat measurements for CeBi_2 indicates that superconductivity in CeBi_2 (and most likely LaBi_2 as well) is not bulk and likely originates from traces of Bi flux, either on the surface of the plate-like samples, or trapped inside the sample as laminar inclusions.

I. INTRODUCTION

Bi-rich compounds manifest a rich variety of ground states. For example, Bi-based families such as ABi ($A = \text{Li}$ and Na)^{1,2}, ABi_2 ($A = \text{K}, \text{Rb}, \text{Cs}$ and Ca)^{3,4} and ABi_3 ($A = \text{Sr}, \text{Ba}, \text{Ca}, \text{Ni}, \text{Co},$ and La) are superconducting (SC) at low temperature^{5–10}. $R\text{Bi}$ ($R = \text{Ce}, \text{Nd}, \text{Tb}$ and Dy) and $R\text{Bi}_2$ ($R = \text{La-Nd}, \text{Sm}$) families have low-temperature magnetic ground states with complex $H-T$ phase diagrams^{11,12}. Moreover, due to the strong spin-orbit coupling of Bi-6*p* electrons they can have substantial ferromagnetic anisotropy, like MnBi ^{13,14}, or, more recently, they have become candidates for realizing novel topological phases, such as topological insulators or topological superconductors^{15–19}.

Among these, the $R\text{Bi}_2$ family displays different magnetic ground states depending on the choice of R ¹². Structurally, $R\text{Bi}_2$ forms in an orthorhombic structure with single layers of Bi separated from each other by $R\text{Bi}$ bilayers that are stacked along the crystallographic b axis^{12,20}. When R is chosen to be the moment-bearing Ce ion, an antiferromagnetic (AFM) ground state below $T_N \sim 3.3$ K can be stabilized¹². A recent study shows that CeBi_2 is a Kondo system with a Sommerfeld coefficient γ over 200 mJ/mol K² and Kondo temperature of an order of ~ 2 K²⁰. On the other hand, for $R = \text{La}$ (non-moment bearing), LaBi_2 reveals metallic behavior without indications of magnetic ordering or superconductivity down to 1.8 K¹².

In this study, we perform a comparative study of the ground-state tunability of these two members by external pressure. We explore the temperature-pressure phase diagram of CeBi_2 and LaBi_2 by resistance measurements and complement these, in case of CeBi_2 , with specific heat measurements. Our results show that T_N of CeBi_2 is moderately increased upon increasing pressure. Surprisingly, resistance measurements of both CeBi_2 and LaBi_2 show signatures pressure-induced superconductivity at low temperature ($T \lesssim 4$ K) above very similar threshold pressures ($p \gtrsim 1.68$ GPa). However, specific heat measurement of CeBi_2 does not reveal any anomaly

that could be associated with a transition into the superconducting state. We assign these effects to filamentary SC that likely originates from traces of Bi flux, either on the surface of the plate-like samples, or trapped inside the sample as laminar inclusions. Finally, the analysis of pressure-dependent resistance data at fixed temperatures for CeBi_2 suggests that there might be a pressure-induced crossover most likely associated with pressure-induced changes in the Kondo temperature and crystal electric field splitting.

II. EXPERIMENTAL DETAILS

Single crystals of CeBi_2 and LaBi_2 were grown by a Bi self-flux technique with the help of a frit-disk alumina Canfield Crucible Set^{21,22}. For CeBi_2 , Ce and Bi in the molar ratio 9:91 were loaded into a crucible set and sealed into a fused silica ampoule under partial argon atmosphere. The ampoule was heated to 1000 °C in 5 h and dwelled at this temperature for another 4 h. It was then slowly cooled to 600 °C over 45 h. At this temperature, the ampoule was removed from the furnace and excess liquid was decanted by the help of a centrifuge. For LaBi_2 , La and Bi in the molar ratio 8:92 were loaded into the crucible set, heated to 1000 °C in 5h, dwelled at 1000 °C for 2 h, and slowly cooled to 350 °C over 80 h. The resulting crystals of CeBi_2 and LaBi_2 are millimeter-size and plate-shaped. Both CeBi_2 and LaBi_2 crystals are air-sensitive, the preparation of experiments was therefore performed in a N_2 glovebox.

The ac , in-plane resistance measurements were performed in a Quantum Design Physical Property Measurement System (PPMS) using a 1 mA excitation with frequency of 17 Hz, on cooling using a rate of - 0.25 K/min. The magnetic field was applied perpendicular to the current direction. For CeBi_2 , two different samples (labeled as S1 and S2) were used in resistance measurements. S1 was measured at ambient condition outside pressure cell and S2 was measured under pressure. The temperature-dependent resistance data for S1 is normalized by extrapolating $p \leq 1.23 \text{ GPa}$ pressure-dependent

resistance data, $R(p)$, at 300 K from S2 back to 0 GPa (see Fig. 1). For LaBi_2 , only one sample was measured under pressure with the pressures $0.60 \text{ GPa} \leq p \leq 2.52 \text{ GPa}$. For both compounds, a standard four-contact configuration was used with contacts made by Dupont 4929N silver paint. Specific heat measurements under pressure were performed using an ac calorimetry technique on a third sample (sample S3) in a cryogen-free cryostat from ICEOxford (Lemon-Dry) with base temperature of 1.4 K. Details of the setup used and the measurement protocol are described in Ref. 23.

In this study, a Be-Cu/Ni-Cr-Al hybrid piston-cylinder cell, similar to the one described in Ref. 24, was used to apply pressure. Good hydrostatic conditions were achieved by using a 4:6 mixture of light mineral oil:n-pentane as pressure medium, which solidifies, at room temperature, in the range 3 – 4 GPa, i.e., well above our maximum pressure^{24–26}. Pressure values were inferred from the $T_c(p)$ of lead²⁷, determined via resistance measurements.

III. RESULTS

A. CeBi_2

Figure 1 shows the temperature-dependent resistance of CeBi_2 at ambient pressure (sample S1) and pressure up to 2.44 GPa (sample S2). The temperature-dependent resistance data for S1 is normalized by extrapolating the 300 K pressure-dependent resistance data ($R(p)$ for $p \leq 1.23 \text{ GPa}$) measured from S2 back to 0 GPa. As shown in the figure, the resistance decreases upon cooling, showing a metallic behavior. At $T \sim 50 \text{ K}$, a broad drop of resistance is observed. In an earlier work, it was suggested that this drop in $R(T)$ is associated with either the coherence in Kondo scattering or crystal electric-field (CEF) splitting of Ce atoms²⁰. At $T \sim 3.3 \text{ K}$, the resistance shows a kink-like anomaly due to loss of spin-disorder scattering as CeBi_2 undergoes an AFM transition at T_N ^{12,20}. Sample S2 was measured under pressure and at lowest pressure (0.12 GPa), resistance of S2 shows very similar feature as S1. Upon increasing pressure, the resistance gradually increases over a large temperature range (essentially everywhere in the paramagnetic state). This is a typical behavior for a Ce-based Kondo lattice under pressure^{28–31}. The broad drop of resistance at ambient pressure becomes progressively more pronounced, as pressure is increased, and evolves into a local maximum at highest pressures. The temperature of this broad drop/hump feature is labeled as T' and indicated by arrow in the figure (see below for the description of the criterion used). The evolution of this feature will be analyzed and discussed in more details below. As we move to the low-temperature region (inset to Fig. 1), for $p \leq 1.23 \text{ GPa}$, the kink-like anomaly, which is associated with the magnetic transition^{12,20}, is shifted to higher temperatures upon increasing pressure. Even with this slight

increase in T_N , the loss of spin disorder scattering below T_N remains fundamentally the same. As a result, the resistance at 1.8 K, $R(1.8 \text{ K})$, does not show a significant change. Upon increasing from 1.23 GPa to 1.68 GPa, $R(1.8 \text{ K})$ shows a sudden decrease. For $p > 1.68 \text{ GPa}$, the resistance as a function of temperature, $R(T)$, undergoes a much sharper drop and reaches a zero value, suggesting a pressure-induced superconducting phase at low temperature. The critical temperature of this phase is increased upon increasing pressure.

The temperature-derivative of the resistance data is shown in Fig. 2 to better differentiate between the low p and high p feature at low temperature as well as to trace the broad feature at $T \sim 50 \text{ K}$. As shown in Fig. 2 (a), at low pressures ($p \leq 1.23 \text{ GPa}$), the magnetic transition shows up as a jump-like feature in the dR/dT . We therefore define T_N as the midpoint of the jump-like feature in dR/dT (see dotted lines and arrow in Fig. 2 (a) as well as Figs. 5 (b) and (c) below). As a result, T_N increases with increasing p with a slope of $\sim 0.48 \text{ K/GPa}$. At higher pressures ($p \geq 1.68 \text{ GPa}$), the superconducting transition can be seen as a sharp peak in dR/dT . Figure 2 (b) shows dR/dT curves over a larger temperature range. As shown in the figure, the broad drop/hump features in $R(T)$ are reflected in minima dR/dT . We therefore define the crossover temperature T' , which marks the change between two different resistance regimes, by the minima in the dR/dT as indicated by the dashed lines in the figure. It is clearly seen that T' increases upon increasing pressure.

To trace the magnetic transition to higher pressures, the temperature-dependent resistance under magnetic fields up to 9 T applied along the b -axis was studied. The applied field can suppress the superconducting transition which masks the signature of the magnetic transition for $p \geq 1.68 \text{ GPa}$. The results for selected pressures are presented in Fig. 3. As shown in Figs. 3 (a) and (c), at 0.12 GPa the kink-like anomaly in $R(T)$ associated with magnetic transition is broadened in higher fields, yet not much shifted with an applied field of 3 T. In the temperature derivative of the resistance data, the corresponding jump-like feature is suppressed with increasing magnetic fields until it disappears at higher fields. At 2.44 GPa, the sharp drop of the resistance in $R(T)$ associated with superconducting transition at $\sim 5 \text{ K}$ is suppressed to lower temperatures with magnetic fields and the kink-like anomaly re-emerges at $\sim 4 \text{ K}$. Further increasing magnetic fields broadens the kink-like anomaly until it disappears. Similarly, in the temperature derivative dR/dT , we first observed a sharp peak associated with the superconducting transition at low magnetic fields. Upon increasing the field, the sharp peak is suppressed and shifted to lower temperatures, at the same time, a second jump-like feature emerges. At even higher fields, both features disappear. By analogy we associate this re-emerged kink-like anomaly in $R(T)$ (jump-like feature in dR/dT) with the same magnetic transition that is observed at low pressures. The resistance does not become

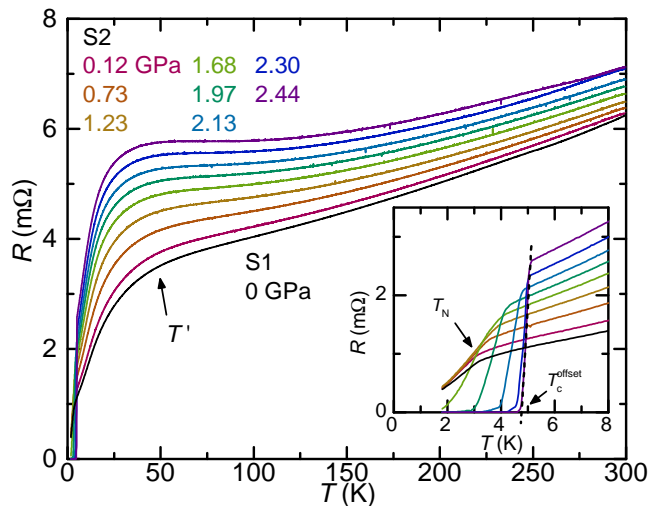


FIG. 1. Resistance of CeBi₂ as a function of temperature at ambient pressure (measured on sample S1) and at different finite pressures up to 2.44 GPa (measured on sample S2). The ambient pressure data for S1 is normalized by extrapolating $p \leq 1.23$ GPa pressure-dependent resistance data, $R(p)$, at 300 K from S2 back to 0 GPa. A broad hump feature is present in all data sets. The inferred crossover temperature T' is exemplarily marked for the data set at 2.44 GPa (for more details, see text). Inset: Blowup of the resistance data at low temperatures showing the magnetic and superconducting transitions. AFM transition temperature T_N is indicated by arrow. Criterion for T_c^{offset} is indicated by arrow.

zero at 1.8 K for magnetic field $B \geq 2$ T indicating a critical field of ~ 2 T at 1.8 K.

To further investigate the overall increase of resistance with pressure, we present in Fig. 4 the pressure dependent resistance $R(p)$ at fixed temperatures. As shown in the figure, a change of slope is observed when pressure is increased from 1.68 GPa to 1.97 GPa at 10 K, this feature persists up to 300 K, the highest temperature investigated in this study. The strongest pressure responses are for $T \lesssim T'$, suggesting shifts in the Kondo feature around T' . Whereas the $R(p)$ data for 300 K are quite similar to what is found for LaBi₂ in Fig. 9 (see below).

The observation of a state with zero resistance in CeBi₂ calls for a thermodynamic investigation of the temperature-pressure phase diagram. Thus, we studied the specific heat of CeBi₂ (sample S3) under pressure and the results are presented in Fig. 5 (a). At lowest pressure (0.04 GPa), very close to ambient pressure, the specific heat, $C_p(T)$, nicely reveals a nearly mean-field-like anomaly at $T \sim 3.2$ K, which speaks in favor of a second-order phase transition. The shape, position, and size of the feature is consistent with the specific results of a previous study and therefore allows us to assign this feature to the magnetic transition at T_N . Figures. 5 (b) and (c) show the comparison between temperature dependent C_p and dR/dT at two sets of nearly identical pressures (0.04 GPa and 0 GPa, 1.28 GPa and 1.23

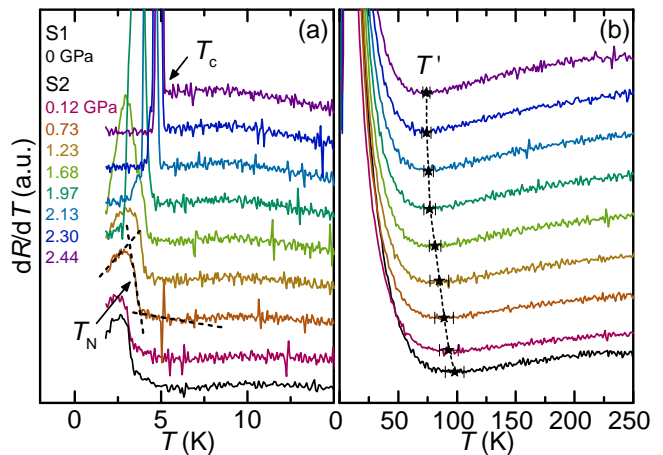


FIG. 2. (a) Temperature derivative of the resistance, dR/dT , in the low-temperature region ($T \leq 15$ K). The criterion for the determination of the AFM transition temperature T_N is illustrated by dashed lines and marked by the arrow (midpoint of the jump-like feature). At high pressures, the magnetic anomaly is masked by a strong drop of resistance, likely due to spurious SC (see main text). The respective temperature is denoted by T_c (see arrow). (b) Temperature derivative of the resistance, dR/dT , showing the evolution of the temperature associated with the broad hump feature in $R(T)$ curves. T' is determined by the minimum in dR/dT curves. Data sets in (a) and (b) are offset for clarity.

GPa). As shown in the figure, temperature-dependent $C_p(T)$ and dR/dT exhibit similar jump-like feature at the transition temperature which is consistent with the Fisher-Langer relation^{32,33}. Thus, to determine the transition temperature, T_N , from specific heat measurement, same criterion as in the resistance measurement is used (midpoint of jump-like anomaly as indicated by dashed lines and arrow in Fig. 5 (a)). As pressure is increased up to 2.55 GPa, T_N is monotonically increased. At the same time, the jump size of the anomaly does not significantly change indicating that the amount of entropy released at T_N is unchanged. However, we did not observe a second feature at any pressure, thus suggesting that CeBi₂ does not undergo any other phase transition than the magnetic one. This includes in particular also a possible superconducting transition for $p > 1.68$ GPa inferred from our resistance data. One might argue that a possible superconducting feature in specific heat is masked by the huge entropy release at the magnetic transition, as T_N and the resistive T_c are very close. However, even at high pressure, at which we expect that T_N and T_c are well separated, no feature in specific heat occurs (see inset of Fig. 5 (a)). Another possibility for the apparent absence of a specific heat feature might be that the superconducting jump size is very small and therefore falls below the resolution limit. In the following, we provide estimates for the lower and upper bound of superconducting jump size in CeBi₂.

For a phonon-mediated BSC superconductor, the spe-

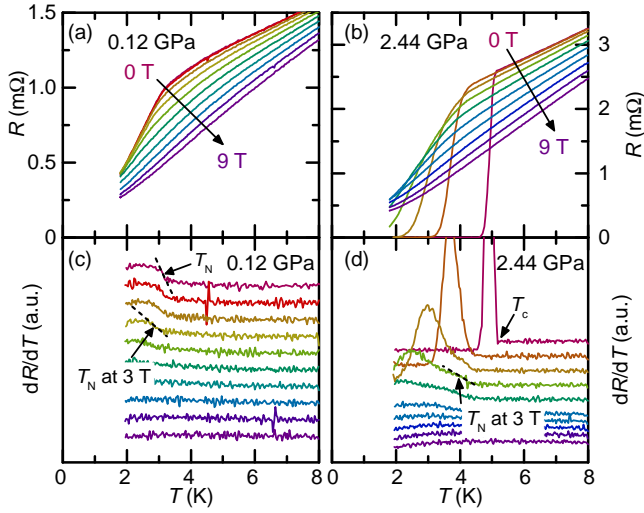


FIG. 3. (a), (b) Temperature-dependent resistance of CeBi₂ S2 under magnetic fields up to 9 T for selected pressures. Fields are applied along the *b*-axis. (c), (d) Temperature-derivative of the resistance data, taken in applied magnetic fields, shown in (a) and (b), respectively. Data sets are offset for clarity. Criteria for T_N at 0 T and 3 T are indicated by arrows (midpoint of the jump-like feature).

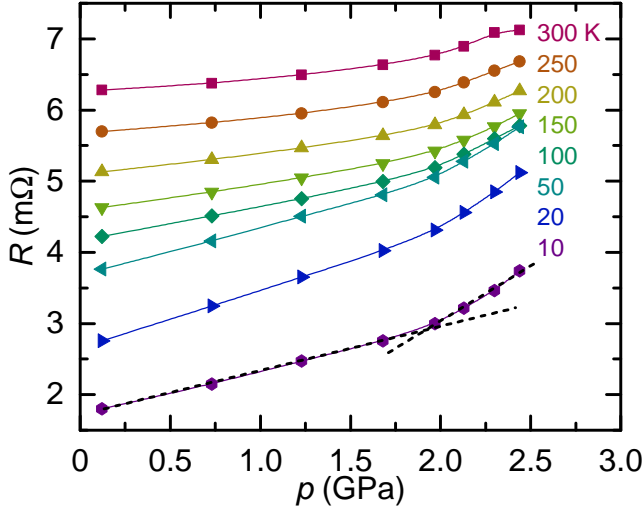


FIG. 4. Pressure dependence of resistance, $R(p)$, at fixed temperatures for CeBi₂. A change of slope between 1.68 GPa and 1.97 GPa is indicated by the cross of the dashed line.

sific heat jump at the superconducting transition can be written as,

$$\Delta C = 1.43\gamma T_c, \quad (1)$$

where γ is the electronic Sommerfeld coefficient and T_c is the superconducting transition temperature. To estimate a possible lower limit of ΔC , we first assume that superconductivity is unrelated to the Kondo-lattice nature of CeBi₂. Thus, for the choice of γ , we refer to the nonmagnetic reference LaBi₂ which is isostructural

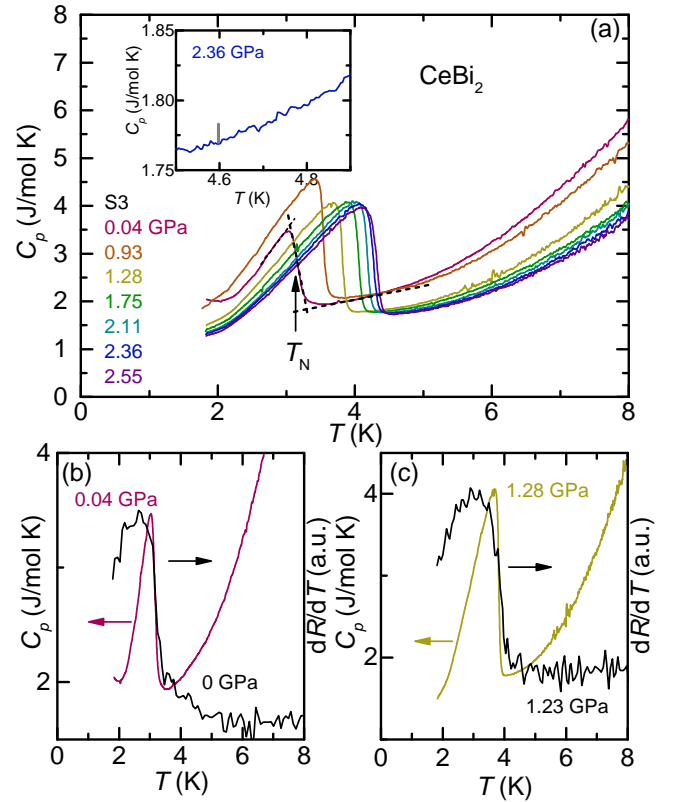


FIG. 5. (a) Evolution of the temperature-dependent specific heat, $C_p(T)$, with pressure up to 2.55 GPa for CeBi₂ S3. Criterion for T_N is indicated by arrow (midpoint of the specific heat jump). The inset shows the data near 4.6 K for 2.36 GPa, the gray vertical line indicates a 13.2 mJ/mol K specific heat jump at 4.6 K (details are discussed in the main text). (b), (c) Temperature-dependent specific heat data and temperature-derivative of the resistance data at two sets of nearly identical pressures ((b) 0.04 GPa and 0 GPa, (c) 1.28 GPa and 1.23 GPa). Note that the midpoint criterion gives same T_N values for both data sets.

to CeBi₂. Since LaBi₂ has a γ value of 2 mJ/mol K²¹², with $T_c \sim 4.6$ K from Fig. 1, we get $\Delta C = 13.2$ mJ/mol K. Compared to the noise level, such value of specific jump (gray vertical line in the inset of Fig. 5 (a)) should be resolvable. For an upper limit, we take the γ value of the Kondo-lattice CeBi₂, 200 mJ/mol K²²⁰, we get $\Delta C = 1.32$ J/mol K, which would be one hundred times larger than the gray vertical line in the inset of Fig. 5 (a). The absence of any resolvable specific heat jump feature, which can be associated with superconductivity, suggests that the pressure-induced superconductivity is likely filamentary rather than bulk. This conclusion will be related to again below after presentation of data on LaBi₂.

We summarize our T_N and T' data for CeBi₂ as well as our T_c^{offset} (filamentary) data in the temperature-pressure ($T-p$) phase diagram shown in Fig. 6. For the magnetic transition, both T_N at zero field and 3 T from resistance measurement (Fig. 3) and T_N from zero field specific

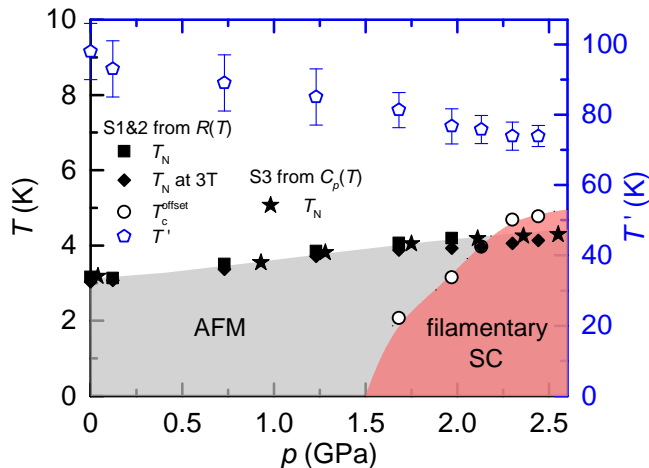


FIG. 6. Temperature-pressure phase diagram of CeBi_2 as determined from resistance and specific heat measurements. Black squares and diamonds represent the magnetic transition T_N determined from resistance measurement for 0 T and 3 T respectively. Black stars represent T_N determined from specific heat measurement. Black open symbols represent the superconducting transition T_c^{offset} determined from resistance measurement. Blue pentagons represent T' determined from resistance measurement (Note the right axis used here for T'). Gray and red areas represent the antiferromagnetically ordered and filamentary-superconducting regions, respectively.

heat data are included. For superconducting transition, T_c^{offset} is determined from resistance measurement (Fig. 1 (b)). The T_N values, inferred from $R(T, p)$ and $C(T, p)$ agree reasonably well within their experimental resolution. As shown in Fig. 6, magnetic field suppresses magnetic transition T_N slightly (~ 0.2 K by 3 T), as is often the case for antiferromagnets. T_N increases monotonically with pressure with a rate of 0.48 K/GPa up to 2.55 GPa. For superconductivity, it first sets in at ~ 1.68 GPa with a sharp drop in $R(T)$, yet not give rise to zero resistance down to 1.8 K. Upon increasing pressure, the drop in $R(T)$ becomes progressively sharper and zero resistance at low temperature is reached as well. Furthermore, from 1.68 GPa to 2.44 GPa, T_c^{offset} monotonically increases from 2.1 K to 4.8 K, appearing to saturate at our highest pressure. Finally, the temperature T' associated with Kondo coherence scattering or CEF splitting is suppressed upon increasing pressure, with $T' \simeq 98$ K at 0 GPa and 74 K at 2.44 GPa.

B. LaBi_2

Next, we discuss our resistance data for the non-magnetic, LaBi_2 , member of the $R\text{Bi}_2$ family. Figure 7 presents the pressure evolution of the temperature-dependent resistance for LaBi_2 with pressures $0.60 \text{ GPa} \leq p \leq 2.52 \text{ GPa}$. For all pressures, resistance decreases upon cooling, showing metallic behavior. For a large

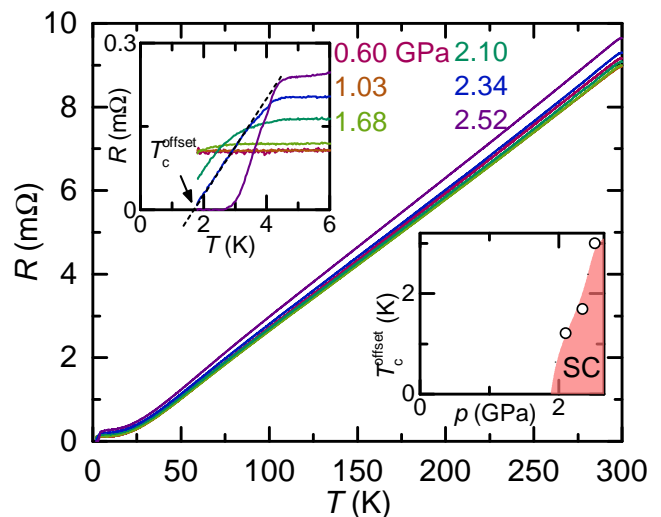


FIG. 7. Resistance of LaBi_2 as a function of temperature at different pressures for $0.60 \text{ GPa} \leq p \leq 2.52 \text{ GPa}$. Upper inset: blowup of the resistance data at low temperatures showing the superconducting transition. Criterion for T_c^{offset} is indicated by arrow. Bottom inset: superconducting transition temperature, T_c^{offset} , as a function of pressure. Red area represent the superconducting region as inferred from resistance measurement.

temperature range ($T \gtrsim 50$ K), the resistance shows linear dependence on temperature. In the low-temperature region (upper inset of Fig. 7), for $p \leq 1.03$ GPa, resistance as a function of temperature is relatively flat suggesting that the low-temperature resistance is dominated by impurity scattering. At 1.68 GPa, $R(T)$ shows a faster drop of resistance below ~ 2.5 K. When pressure is further increased, this drop of resistance becomes more pronounced. At 2.52 GPa, resistance actually drops to zero below 2.7 K, suggesting pressure-induced superconductivity. The drop of resistance, visible for $1.68 \text{ GPa} \leq p \leq 2.34 \text{ GPa}$, is likely to be associated with traces of superconducting phase. Using the criterion defined in the upper inset of Fig. 7, the superconducting transition temperature, T_c^{offset} , can be traced and the results are shown in the bottom inset of Fig. 7. As shown in the figure, T_c^{offset} increases from 1.2 K to 3 K when pressure is increased from 2.10 GPa to 2.52 GPa.

The field dependence of the resistance at 2 K was studied and is presented in Fig. 8. For $p \leq 1.03$ GPa, resistance gradually increases with magnetic field with a slightly up-bending curvature. For $p \geq 1.68$ GPa, at low fields, the resistance first undergoes a fast increase upon increasing fields, which is likely due to the suppression of superconductivity. At higher fields, $R(H)$ curves behave similarly with the ones at lower pressures. Moreover, at 2.52 GPa the zero resistance at 2 K is lifted for $H \gtrsim 500$ Oe, indicating a critical field of ~ 500 Oe. Bearing in mind that close to ambient pressure the magnetoresistance clearly deviates from the conventional H^2 behavior, we observe that pressures up to ~ 2.5 GPa do not

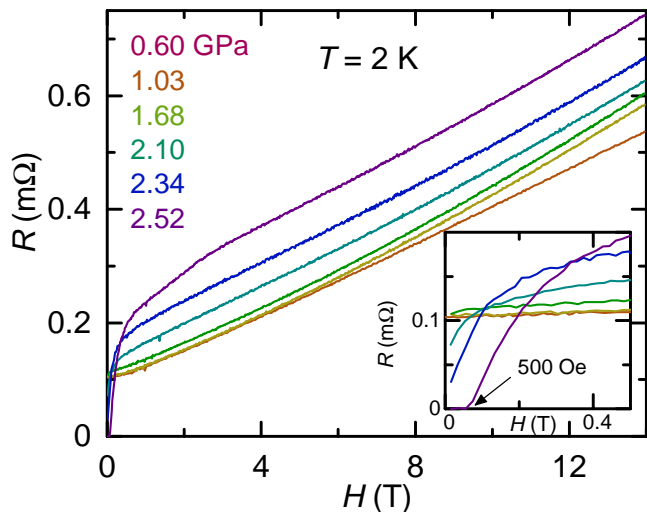


FIG. 8. Evolution of the field-dependent resistance at 2 K of LaBi₂ with pressure 0.60 GPa $\leq p \leq$ 2.52 GPa and fields applied along the b -axis. The lowest pressure data (0 GPa) is not included due to excessive noise. Inset shows the blowups of the low-field region.

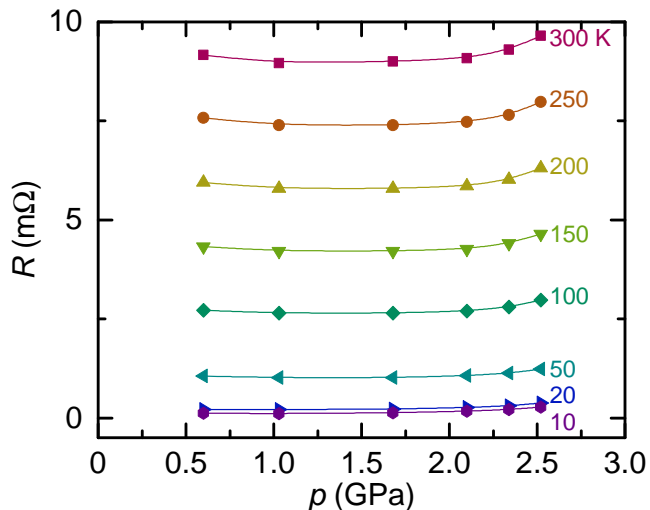


FIG. 9. Pressure dependence of resistance, $R(p)$, at fixed temperatures for LaBi₂. The lowest pressure data (0 GPa) is not included due to excessive noise.

modify this behavior (besides the lower field effects of superconductivity) in any conspicuous way. The data in Figs. 7 and 8 are consistent with traces of SC phase, with distributions of T_c values existing in the LaBi₂ sample. The mean T_c of these filamentary traces increases with pressure for $p > 1.68$ GPa.

To better visualize the pressure evolution of the higher temperature resistance for LaBi₂, Fig. 9 presents the pressure-dependent resistance $R(p)$ at fixed temperatures. The resistance of LaBi₂ first decreases and then increases with pressure, giving rise to a broad minimum between 1.03 GPa and 1.68 GPa. Compared with the $R(p)$

of CeBi₂, $R(p)$ of LaBi₂ has a similar higher-pressure, higher-temperature up-turn, but lacks the larger $T \lesssim T'$ pressure dependence seen in CeBi₂.

IV. DISCUSSION

Before discussing the implications of the zero-resistive state, which we observed in CeBi₂ and LaBi₂ at higher pressures, we first focus on the increase of T_N and decrease of T' under pressure in CeBi₂, as this is robustly established by our resistance and specific heat study. The properties of a Kondo lattice system are usually dominated by two characteristic energy scales, which are both susceptible to externally applied pressure: Ruderman-Kittel-Kasuya-Yosida (RKKY) interaction energy $T_{\text{RKKY}} \propto J^2$ and Kondo interaction energy $T_K \propto e^{-1/J}$ where J is the exchange interaction^{34–38}. When $T_{\text{RKKY}} \gg T_K$, the ground state is magnetic and for $T_K \gg T_{\text{RKKY}}$, it is nonmagnetic. The competition between them and the resulting ground state is often described by the Doniach phase diagram³⁹. For Ce-based compounds, the ground state is often magnetic. Applying external pressure can suppress magnetic transition temperature to zero and lead to non-magnetic ground state via a quantum critical point^{40–45}. In our study, the AFM transition temperature T_N of CeBi₂ is moderately increased by pressure up to ~ 2.5 GPa. This suggests that at ambient pressure, CeBi₂ is deeply in its magnetic state and higher pressure is needed to suppress T_N ^{46–49}. This is compatible with the Doniach picture, as there is a maximum of T_N due to the explicit functional dependences of T_{RKKY} and T_K . Moreover, in the Doniach picture, when pressurizing a Ce-based Kondo lattice, an increase of T_K is often observed due to the enhancement of exchange interaction J ^{28,50}. This, in turn, should give rise to a shift of broad resistive features, associated with T_K , to higher temperatures with pressure. Therefore, a suppression of T' observed in this study suggests that the broad drop/hump feature in $R(T)$ can not be explained by only the Kondo coherence scattering^{29,31,51}.

The resistance measurements for both CeBi₂ and LaBi₂ reveal a zero-resistive state at high pressures, suggesting a pressure-induced SC phase for these compounds. By comparing their $T - p$ phase diagrams (Figs. 6 and 7 (a) inset), we see that the two phase diagrams exhibit similar SC phase regions, but with slightly different onset pressures and T_c values. For CeBi₂ T_c saturated at ~ 4.8 K by 2.44 GPa whereas T_c of LaBi₂ reaches ~ 3 K but seems still rising with pressure. Moreover, at the highest pressures in this study (2.44 GPa for CeBi₂ and 2.52 GPa for LaBi₂), CeBi₂ and LaBi₂ have very different critical fields at ~ 2 K (~ 2 T for CeBi₂ and ~ 500 Oe for LaBi₂).

Despite the zero-resistive state and relative sharp resistance drop at high pressures for CeBi₂ and LaBi₂, we would like to argue that the observed SC feature is extrinsic for the following reasons. First of all, specific heat

measurement under pressure for CeBi₂ does not reveal any SC feature which strongly speaks in favor of filamentary SC. Second, similar T_c values for Ce and La are unlikely in bulk $R\text{Bi}_2$. On one hand, if the SC in these two compounds is standard BSC SC, then hybridizing rare earths such as Ce or Yb suppresses T_c aggressively⁵²⁻⁵⁴. On the other hand, if CeBi₂ at high pressures becomes a heavy fermion superconductor, the specific heat jump anomaly at T_c should be even bigger. Then similar SC onset pressure and T_c between LaBi₂ and CeBi₂ are unlikely again as LaBi₂ is not a heavy fermion compound.

To speculate about the possible origin of the filamentary SC, we refer to literature. First we notice that similar situation has been found in other Bi compounds as well where SC is attributed to Bi flux or thin films of Bi⁵⁵⁻⁵⁷. Moreover, it is known that single-crystalline Bi undergoes sequential structural transitions upon increasing pressure and possesses rich physics under pressure⁵⁸⁻⁶⁰. Specifically, at low temperature, Bi-II exists between 2.55 GPa and 2.70 GPa with $T_c \sim 3.9$ K and upper critical field $\mu_0 H_{c2}(2\text{ K}) \sim 0.05$ T, Bi-III exists between 2.70 GPa and 7.7 GPa with $T_c \sim 7$ K and $\mu_0 H_{c2}(2\text{ K}) \sim 3$ T⁶⁰. Owing to the very similar T_c of Bi-II to our results on CeBi₂ in the almost identical pressure range, we suspect that the filamentary SC we observed in the resistance measurement of CeBi₂ originates from traces of Bi flux. It is likely that the SC in LaBi₂ is non-bulk and originates from Bi flux as well. Slight differences in onset pressure and $\mu_0 H_{c2}$ could arise from details of the unit cell parameters which could give rise to slightly different strain conditions.

V. CONCLUSION

In conclusion, the resistance of $R\text{Bi}_2$ ($R = \text{La}$ and Ce) under pressure up to ~ 2.5 GPa and ac specific heat of CeBi₂ under pressure up to 2.55 GPa have been studied. Our studies show that for CeBi₂ the antiferromagnetic transition temperature, T_N , increases upon increasing pressure with the rate of ~ 0.48 K/GPa. This fits into the Doniach phase diagram and suggests that there might be a maximum of T_N , followed by its decrease and finally a quantum critical point at possibly significantly higher pressures. Resistance and ac specific heat measurements of CeBi₂ together suggest that the pressure-induced superconductivity in CeBi₂ is likely not bulk. It is likely that the SC phase is filamentary Bi either on the surface or as laminar in the bulk of the sample. We suspect the pressure-induced superconductivity in LaBi₂ to arise from a similar extrinsic origin giving that the onset pressure and transition temperature of superconductivity are very similar to that of CeBi₂. Further pressure-dependent resistance analyses for CeBi₂ and LaBi₂ indicate some anomalies in the $R(p)$ curves, a change of slope between 1.68 GPa and 1.97 GPa for CeBi₂ and a broad minimum between 1.03 GPa and 1.68 GPa for LaBi₂. Taken together, these suggest that the stronger,

low-temperature features seen near and below T' for CeBi₂ are related to the pressure dependent hybridization and crystal electric field splitting of the Ce.

Finally, we would like to point out, again, that when studying the properties of Bi-rich compounds under pressure, one needs to be very careful and mindful for the various phases elemental Bi has and the rich physics they display at different pressures⁵⁸⁻⁶⁰.

ACKNOWLEDGMENTS

Work at the Ames Laboratory was supported by the U.S. Department of Energy, Office of Science, Basic Energy Sciences, Materials Sciences and Engineering Division. The Ames Laboratory is operated for the U.S. Department of Energy by Iowa State University under Contract No. DEAC0207CH11358. L.X. was supported, in part, by the W. M. Keck Foundation and the Gordon and Betty Moore Foundations EPiQS Initiative through Grant GBMF4411.

- * ives@iastate.edu
- ¹ T. Sambongi, *J. Phys. Soc. Jpn.* **30**, 294 (1971).
 - ² S. K. Kushwaha, J. W. Krizan, J. Xiong, T. Klimczuk, Q. D. Gibson, T. Liang, N. P. Ong, and R. J. Cava, *Journal of Physics: Condensed Matter* **26**, 212201 (2014).
 - ³ B. W. Roberts, *Journal of Physical and Chemical Reference Data* **5**, 581 (1976).
 - ⁴ M. J. Winiarski, B. Wiendlocha, S. Gob, S. K. Kushwaha, P. Winiewski, D. Kaczorowski, J. D. Thompson, R. J. Cava, and T. Klimczuk, *Phys. Chem. Chem. Phys.* **18**, 21737 (2016).
 - ⁵ B. T. Matthias and J. K. Hulm, *Phys. Rev.* **87**, 799 (1952).
 - ⁶ D. F. Shao, X. Luo, W. J. Lu, L. Hu, X. D. Zhu, W. H. Song, X. B. Zhu, and Y. P. Sun, *Scientific Reports* **6**, 21484 (2016).
 - ⁷ T. Kinjo, S. Kajino, T. Nishio, K. Kawashima, Y. Yanagi, I. Hase, T. Yanagisawa, S. Ishida, H. Kito, N. Takeshita, K. Oka, H. Eisaki, Y. Yoshida, and A. Iyo, *Superconductor Science and Technology* **29**, 03LT02 (2016).
 - ⁸ L. Xiang, R. A. Ribeiro, U. S. Kaluarachchi, E. Gati, M. C. Nguyen, C.-Z. Wang, K.-M. Ho, S. L. Bud'ko, and P. C. Canfield, *Phys. Rev. B* **98**, 214509 (2018).
 - ⁹ E. Gati, L. Xiang, L.-L. Wang, S. Manni, P. C. Canfield, and S. L. Bud'ko, *Journal of Physics: Condensed Matter* **31**, 035701 (2018).
 - ¹⁰ S. Tenc, O. Janson, C. Krellner, H. Rosner, U. Schwarz, Y. Grin, and F. Steglich, *Journal of Physics: Condensed Matter* **26**, 395701 (2014).
 - ¹¹ N. Nereson and G. Arnold, *Journal of Applied Physics* **42**, 1625 (1971).
 - ¹² C. Petrovic, S. L. Bud'ko, and P. C. Canfield, *Journal of Magnetism and Magnetic Materials* **247**, 270 (2002).
 - ¹³ A. Isaeva, B. Rasche, and M. Ruck, *Phys. Status Solidi RRL* **7**, 39 (2013).
 - ¹⁴ V. Taufour, S. Thimmaiah, S. March, S. Saunders, K. Sun, T. N. Lamichhane, M. J. Kramer, S. L. Bud'ko, and P. C. Canfield, *Phys. Rev. Applied* **4**, 014021 (2015).
 - ¹⁵ M. Z. Hasan and C. L. Kane, *Rev. Mod. Phys.* **82**, 3045 (2010).
 - ¹⁶ X.-L. Qi and S.-C. Zhang, *Rev. Mod. Phys.* **83**, 1057 (2011).
 - ¹⁷ Y. S. Hor, A. J. Williams, J. G. Checkelsky, P. Roushan, J. Seo, Q. Xu, H. W. Zandbergen, A. Yazdani, N. P. Ong, and R. J. Cava, *Phys. Rev. Lett.* **104**, 057001 (2010).
 - ¹⁸ Y. Xia, D. Qian, D. Hsieh, L. Wray, A. Pal, H. Lin, A. Bansil, D. Grauer, Y. S. Hor, R. J. Cava, and M. Z. Hasan, *Nature Physics* **5**, 398 (2009).
 - ¹⁹ Y. L. Chen, J. G. Analytis, J.-H. Chu, Z. K. Liu, S.-K. Mo, X. L. Qi, H. J. Zhang, D. H. Lu, X. Dai, Z. Fang, S. C. Zhang, I. R. Fisher, Z. Hussain, and Z.-X. Shen, *Science* **325**, 178 (2009).
 - ²⁰ W. Zhou, C. Q. Xu, B. Li, R. Sankar, F. M. Zhang, B. Qian, C. Cao, J. H. Dai, J. Lu, W. X. Jiang, D. Qian, and X. Xu, *Phys. Rev. B* **97**, 195120 (2018).
 - ²¹ P. C. Canfield and Z. Fisk, *Philosophical Magazine B* **65**, 1117 (1992).
 - ²² P. C. Canfield, T. Kong, U. S. Kaluarachchi, and N. H. Jo, *Philosophical Magazine* **96**, 84 (2016).
 - ²³ E. Gati, G. Drachuck, L. Xiang, L.-L. Wang, S. L. Bud'ko, and P. C. Canfield, *Review of Scientific Instruments* **90**, 023911 (2019).
 - ²⁴ S. L. Bud'ko, A. N. Voronovskii, A. G. Gapotchenko, and E. S. Itskevich, *Zh. Eksp. Teor. Fiz.* **86**, 778 (1984).
 - ²⁵ S. K. Kim, M. S. Torikachvili, E. Colombier, A. Thaler, S. L. Bud'ko, and P. C. Canfield, *Phys. Rev. B* **84**, 134525 (2011).
 - ²⁶ M. S. Torikachvili, S. K. Kim, E. Colombier, S. L. Bud'ko, and P. C. Canfield, *Rev. Sci. Instrum.* **86**, 123904 (2015).
 - ²⁷ B. Bireckoven and J. Wittig, *Journal of Physics E: Scientific Instruments* **21**, 841 (1988).
 - ²⁸ J. D. Thompson and J. M. Lawrence, in *Handbook on the Physics and Chemistry of Rare Earths*, Vol. 19 (Elsevier, 1994) pp. 383–478.
 - ²⁹ H. Hegger, C. Petrovic, E. G. Moshopoulou, M. F. Hundley, J. L. Sarrao, Z. Fisk, and J. D. Thompson, *Phys. Rev. Lett.* **84**, 4986 (2000).
 - ³⁰ M. Nicklas, R. Borth, E. Lengyel, P. G. Pagliuso, J. L. Sarrao, V. A. Sidorov, G. Sparn, F. Steglich, and J. D. Thompson, *Journal of Physics: Condensed Matter* **13**, L905 (2001).
 - ³¹ M. Nicklas, V. A. Sidorov, H. A. Borges, P. G. Pagliuso, C. Petrovic, Z. Fisk, J. L. Sarrao, and J. D. Thompson, *Phys. Rev. B* **67**, 020506(R) (2003).
 - ³² M. E. Fisher and J. S. Langer, *Phys. Rev. Lett.* **20**, 665 (1968).
 - ³³ S. Alexander, J. S. Helman, and I. Balberg, *Phys. Rev. B* **13**, 304 (1976).
 - ³⁴ M. A. Ruderman and C. Kittel, *Phys. Rev.* **96**, 99 (1954).
 - ³⁵ T. Kasuya, *Progress of Theoretical Physics* **16**, 45 (1956).
 - ³⁶ K. Yosida, *Phys. Rev.* **106**, 893 (1957).
 - ³⁷ J. Kondo, *Progress of Theoretical Physics* **32**, 37 (1964).
 - ³⁸ A. C. Hewson, *The Kondo Problem to Heavy Fermions*, Cambridge Studies in Magnetism (Cambridge University Press, 1993).
 - ³⁹ S. Doniach, *Physica B & C* **91**, 231 (1977).
 - ⁴⁰ F. Steglich, J. Aarts, C. D. Bredl, W. Lieke, D. Meschede, W. Franz, and H. Schäfer, *Phys. Rev. Lett.* **43**, 1892 (1979).
 - ⁴¹ D. Jaccard, K. Behnia, and J. Sierro, *Physics Letters A* **163**, 475 (1992).
 - ⁴² N. D. Mathur, F. M. Grosche, S. R. Julian, I. R. Walker, D. M. Freye, R. K. W. Haselwimmer, and G. G. Lonzarich, *Nature* **394**, 39 (1998).
 - ⁴³ T. Park, F. Ronning, H. Q. Yuan, M. B. Salamon, R. Movshovich, J. L. Sarrao, and J. D. Thompson, *Nature* **440**, 65 (2006).
 - ⁴⁴ G. Knebel, D. Aoki, D. Braithwaite, B. Salce, and J. Flouquet, *Phys. Rev. B* **74**, 020501(R) (2006).
 - ⁴⁵ L. Jiao, Y. Chen, Y. Kohama, D. Graf, E. D. Bauer, J. Singleton, J.-X. Zhu, Z. Weng, G. Pang, T. Shang, J. Zhang, H.-O. Lee, T. Park, M. Jaime, J. D. Thompson, F. Steglich, Q. Si, and H. Q. Yuan, *Proc Natl Acad Sci USA* **112**, 673 (2015).
 - ⁴⁶ G. Knebel, D. Aoki, D. Braithwaite, B. Salce, and J. Flouquet, *Phys. Rev. B* **74**, 020501(R) (2006).
 - ⁴⁷ G. F. Chen, K. Matsubayashi, S. Ban, K. Deguchi, and N. K. Sato, *Phys. Rev. Lett.* **97**, 017005 (2006).
 - ⁴⁸ N. Kimura, Y. Muro, and H. Aoki, *J. Phys. Soc. Jpn.* **76**, 051010 (2007).
 - ⁴⁹ E. D. Bauer, H. O. Lee, V. A. Sidorov, N. Kurita, K. Gofryk, J.-X. Zhu, F. Ronning, R. Movshovich, J. D. Thompson, and T. Park, *Phys. Rev. B* **81**, 180507(R) (2010).

- (2010).
- ⁵⁰ A. V. Goltsev and M. M. Abd-Elmeguid, *Journal of Physics: Condensed Matter* **17**, S813 (2005).
- ⁵¹ T. Muramatsu, N. Tateiwa, T. Kobayashi, K. Shimizu, K. Amaya, D. Aoki, H. Shishido, Y. Haga, and Y. Ōnuki, *J. Phys. Soc. Jpn.* **70**, 3362 (2001).
- ⁵² M. B. Maple, W. A. Fertig, A. C. Mota, L. E. DeLong, D. Wohlleben, and R. Fitzgerald, *Solid State Communications* **11**, 829 (1972).
- ⁵³ P. C. Canfield, P. L. Gammel, and D. J. Bishop, *Physics Today* **51**, 10, 40 (1998).
- ⁵⁴ S. L. Bud'ko and P. C. Canfield, *C. R. Physique* **7**, 56 (2006).
- ⁵⁵ A. Thamizhavel, A. Galatanu, E. Yamamoto, T. Okubo, M. Yamada, K. Tabata, T. C Kobayashi, N. Nakamura, K. Sugiyama, K. Kindo, T. Takeuchi, R. Settai, and Y. Ōnuki, *J. Phys. Soc. Jpn.* **72**, 2632 (2003).
- ⁵⁶ H. Mizoguchi, S. Matsuishi, M. Hirano, M. Tachibana, E. Takayama-Muromachi, H. Kawaji, and H. Hosono, *Phys. Rev. Lett.* **106**, 057002 (2011).
- ⁵⁷ X. Lin, W. E. Straszheim, S. L. Bud'ko, and P. C. Canfield, *Journal of Alloys and Compounds* **554**, 304 (2013).
- ⁵⁸ W. Klement, A. Jayaraman, and G. C. Kennedy, *Phys. Rev.* **131**, 632 (1963).
- ⁵⁹ O. Degtyareva, M. I. McMahon, and R. J. Nelmes, *High Pressure Research* **24**, 319 (2004).
- ⁶⁰ Y. Li, E. Wang, X. Zhu, and H.-H. Wen, *Phys. Rev. B* **95**, 024510 (2017).